Multi-regression prediction model for surface roughness and tool wear in turning novel aluminum alloy (LM6)/fly ash composite using response surface and central composite design methodology

Smita Rani Panda[a], Ajit Kumar Senapati[b] and Purna Chandra Mishra[b*]

[a]*Department of Mechanical Engineering, Rajdhani Engineering College, Bhubaneswar, Odisha, India*
[b]*School of Mechanical Engineering, KIIT University, Bhubaneswar - 751024, Odisha, India*

C H R O N I C L E	A B S T R A C T
	Turning experiments were conducted on a novel aluminum alloy (LM6)/fly ash composite based on the response surface and face centered central composite design methodology. The effects of cutting parameters on surface roughness and tool wear were investigated. Multiple regression models were developed for the responses and the adequacies of the developed models were tested at 95% confidence interval using the analysis of variance (ANOVA) technique. Carbide inserts (Model: CNMG 120408-M5) were used for turning the specimens in a CNC turning machine (model: LT-16). The test for significance of the regression models, the test for significance on individual model coefficients and the lack-of-fit tests were performed using the statistical Design-Expert7.0v software environments. R2 indicated the model significance and the value was more than 97%, revealed that the relation between cutting responses and input parameters held good for more than 97% and the model was adequate.

1. Introduction

Waste fly ash reinforced aluminum matrix composites (AMC) are significant for their light weight, superior tribological properties, low material costs, savings in ash disposal costs, energy savings, environmental benefits and good corrosion resistance behavior (Rohatgi et al., 2006), for which they are increasingly being used in automobile, marine and aerospace industries (Anasyida et al., 2010).Due to some enormous properties like high wear resistance, low thermal expansion coefficient, good corrosion resistance, and improved mechanical properties at a wide range of temperatures, the Al-Si alloy was normally selected as matrix material (Saheb et al., 2001). Some researchers evaluated the mechanical properties (Rohatgi et al., 2002; Bienias et al., 2003; Zuoyong Dou et al., 2007), thermal properties (Rohatgi et al., 2006), damping properties (Wu et al., 2006) and tribological properties (Surappa, 2008) with the use of fly ash as reinforcement in aluminum matrix composites (Senapati et al., 2015). However, these are difficult-to-machine materials due to the presence of very hard and brittle reinforcements, which

* Corresponding author. Tel.: +91 674 6540805 (O)
E-mail: pcmishrafme@kiit.ac.in   (P. C. Mishra)

also leads to their poor machinability involving high tool wear and surface imperfections (Li & Seah, 2001;Manna & Bhattacharyya, 2005). Sahoo et al. (2013) presented the development of Al/SiCp (10%weight) metal matrix composite through a conventional casting process and studied its machinability characteristics in turning using multi-layer TiN coated carbide insert under dry environment based on Taguchi'sL9 orthogonal array. Abrasion was found to be the dominant wear mechanism from the experimental study. Udaya Prakash et al. (2013) investigated the effect of parameters like gap voltage, pulse on time, pulse off time, wire feed and percentage of reinforcement on the response material removal rate as well as surface roughness while machining Al413/fly ash/boron carbide hybrid composite using wire electrical discharge machining. Shanmugha Sundaram and Subramanian (2013) experimentally investigated on the surface roughness of pure commercial Al, Al-15 wt% fly ash, and Al- 15 wt% fly ash/1.5 wt% graphite (Gr) composites produced by modified two-step stir casting. The effect of reinforcements and machining parameters such as cutting speed, feed rate, and depth of cut on surface roughness, which greatly influence the performance of the machined product, were analyzed during turning operation. Rao et al., (2014) investigated the machining behavior of Al6061-flyash composite in Jobber XL CNC by using M2 grade HSS and K10 grade carbide inserts as cutting tools. The investigated result conclude that the increased fly ash content in the composites of Al6061 reduces the premature failure of the cutting tool by reducing built up edge formation. K10 grade carbide insert cutting tool is preferred for machining of the Al6061-flyash than that of M2 grade HSS. Charles et al., (2006) developed a mathematical model for machining of hybrid aluminum composites reinforced with SiC and fly ash particles using five level factorial design concepts. They used analysis of variance (ANOVA) technique to calculate the regression coefficients as well as to check the significance of the developed model. They observed that surface roughness increased with increasing the vol. % of SiC particles and current but decreased with increase in pulse duration. Banerjee et al., (2008) used a face centered central composite design approach to develop a mathematical model for material removal rate and surface roughness. A total eighteen experiments were conducted based on the design matrix and the model was found to be adequate. According to the model developed, the surface roughness increased when the pulse on time was increased. Mishra et al., (2015) reported the ANOVA results for grey relational grade indicated that feed was the only significant machining process parameter for the multi-response characteristics under consideration.

This paper describes the mathematical model developed by Multiple Linear Regression Analysis to predict the machinability characteristics at 95% confidence level by response surface and face centered central composite methodology. The results are analyzed using ANOVA technique, i.e. average surface roughness (Ra)and tool wear (VB_c), while turning the composite in dry environment for the same machining parameters.

2. Materials & Methods

Aluminum-silicon alloy(LM6) matrix composite reinforced with 15 wt. % flyash (of average particle size 19.338 μm) was used as work material for turning. Chemical composition test result of the matrix alloy and reinforcement are shown in Table 1 and Table 2.

Table 1
Composition of Al-Si alloy [wt. %] designated as matrix

Si	Co	Fe	Cu	Mn	Ti	Zn	Ni	Sn	Cr	Ca	V	Al
12.25	0.0174	0.4353	0.08	0.1601	0.0672	0.0944	0.0264	0.0632	0.0199	0.0082	0.0146	86.7654

Table 2
Chemical composition of waste fly ash collected from thermal power plant

Compound	SiO_2	Al_2O_3	Fe_2O_3	CaO	MgO	Na_2O	K_2O
(Wt. %)	63.34	24.60	4.97	1.23	0.56	0.11	0.64

For the as received flyash, the micrograph measured by Scanning Electron Microscope (Make: JEOL, Model: JSM-6480LV) and particle size measured by particle size analyzer, (Make: Malvern, Model Micro-P) as shown in Fig.1.

(a)   (b)
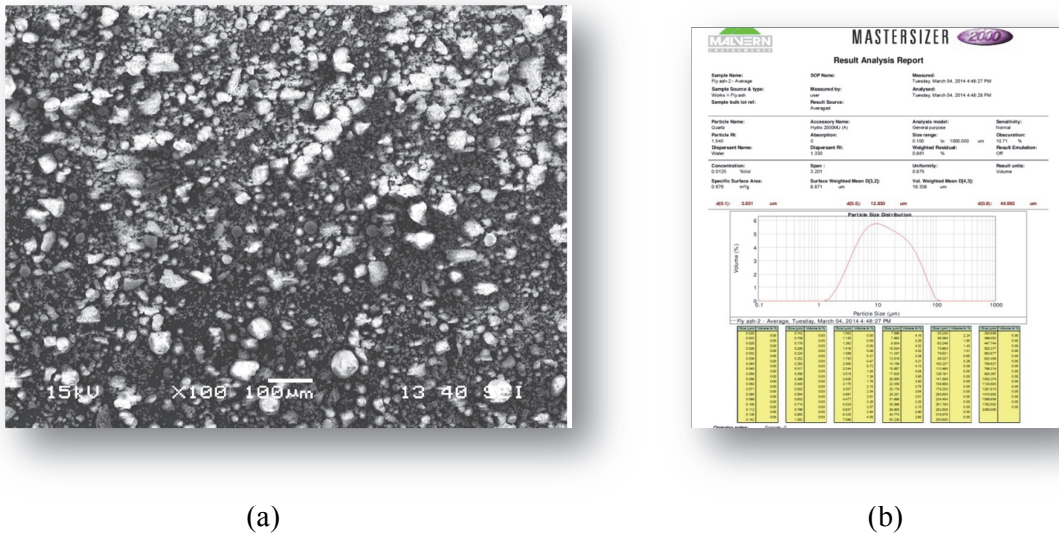
Fig. 1. (a) SEM micrograph and (b) Particle size analysis of as received waste flyash

(a)   (b)   (c)

(d)
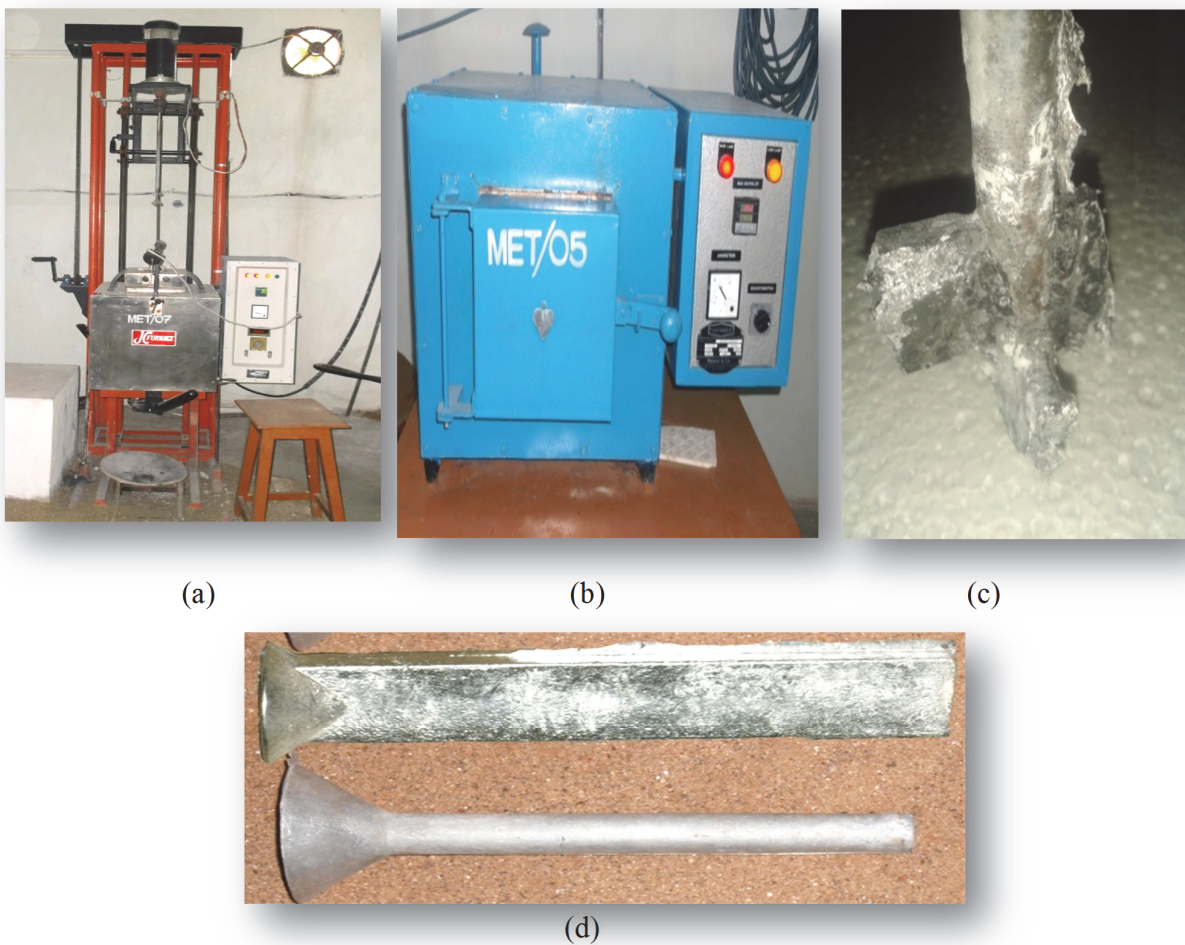
Fig. 2. The components of composite fabrication (a) bottom pouring furnace, (b) muffle furnace, (c) BN coated stainless steel stirrer and (d) cast composite

4

The composite was fabricated by conventional stir casting method in an electrical resistance furnace, mounted with a speed regulated stirring system and temperature controller. The components of the composite fabrication setup are shown in Fig. 2. As received Al-Si alloy ingots were cleaned properly to eliminate the surface impurities and cut into proper sizes. The proper sizes of Al-Si alloy are weighed in requisite quantities and are charged into a vertically aligned pit type bottom poured melting furnace. Flyash was preheated to $650^0C \pm 5^0C$ before pouring in to the melt of aluminum-silicon alloy by using muffle furnace to remove residual moisture and to improve wetability. The pit type bottom pouring furnace temperature was first raised above the liquidus temperature of Al-Si alloy near about 750^0C to melt the Al-Si alloy completely and was then cooled down just to below the liquidus to keep the slurry in semi-solid state. An argon atmosphere was maintained in the furnace throughout the process so as to avoid the pre-oxidation. The molten metal was stirred with a boron nitride (BN) coated stainless steel rotor at a speed of 600-650 rpm.

(a)

(b)

(d)

(c)

(e)
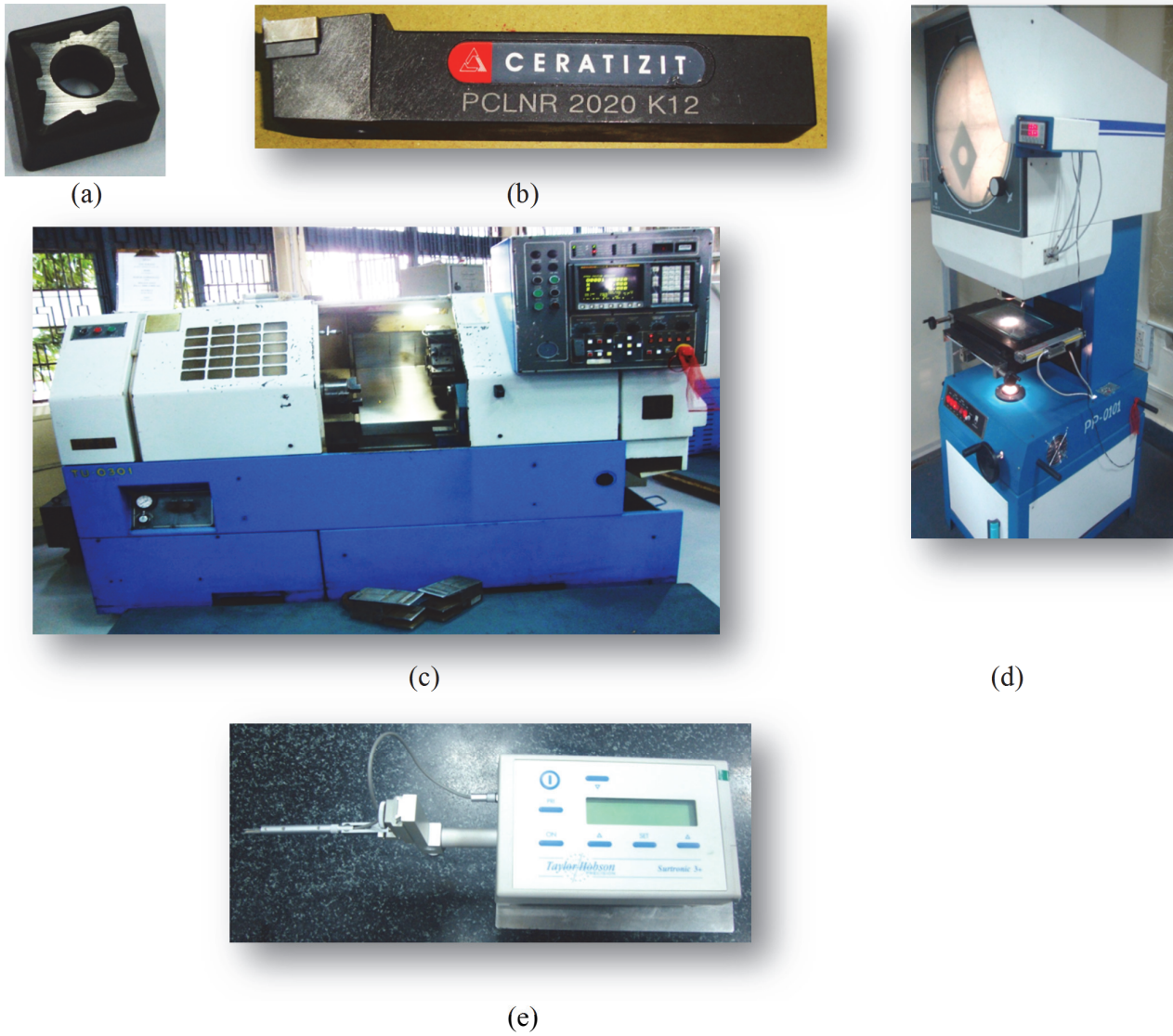
Fig. 4. The components of machining setup (a) carbide insert (CNMG 120408-M5), (b) tool holder (PCLNR2020K12), (c) CNC Lathe (Model LT-16 CNC), (d) Tool Profile Projectors (PP 400 TE) and (e) surface roughness tester (Taylor Hobson, Surtronic 3+).

A vortex was created in the melt because of stirring where the preheated flyash was poured centrally into the vortex. The rotor is moved down slowly, from top to bottom by maintaining clearance of 12 mm from

the bottom. The rotor was then pushed back slowly to its initial position. The pouring temperature of the liquid is kept around 700^0C.Casting was made in cylindrical (i.e, diameter: 30mm and length: 300mm metal moulds. The melt was allowed to solidify in the moulds and cooled to room temperature. Scanning electron microscopy (SEM) graph along with energy dispersive X-ray spectroscopy (EDAX) analysis confirms the presence of unreacted carbon in the matrix as shown in Fig.3. A notable difference is observed in optical micro graphs of virgin Al-Si alloy and AMC reinforced with fly ash. Turning experiments were conducted by a CNC lathe(Make: ACE Designers, Model LT-16) with an accuracy level of 10 microns and carbide inserts of geometry CNMG 120408-M5, manufactured by SECO where main composition is tungsten carbide 94% WC and cobalt 6% Co as binder. The inserts are rigidly mounted on a right hand style tool holder designated by ISO as PCLNR2020K12.Experiments were conducted in dry machining environments. Fig. 4 depicts the turning setup in dry machining environment. Machining process parameters and their levels used for turning the composite are presented in Table 3.

Table 3
Design layout of independent variables and their levels for machinability studies

Process variables	Notation	Unit	Levels				
			$-\alpha$	-1	0	$+1$	$+\alpha$
Cutting Speed	s	m/min	70	90	120	150	170
Feed rate	f	mm/rev	0.02	0.07	0.14	0.21	0.26
Depth of cut	d	mm	0.06	0.20	0.40	0.60	0.74

3. Design of experiments

In machining, the influence of cutting speed, feed rate and depth of cut on cutting tool wear behavior of virgin Al-Si alloy and metal matrix composite prepared with fly ash was investigated. The turning experiments were conducted based upon the combined response surface (RS) and face centered Central Composite Design (CCD) methodology. In the response surface methodology (RSM), the quantitative form of relationship between desired response and independent input parameters could be represented as (Montgomery, 1990).

$$y = f(x_1, x_2, x_3, \ldots x_n) \pm err \, , \tag{1}$$

where y is the desired response, f is the response function (or response surface), $x_1, x_2, x_3\ldots x_n$ are the independent input parameters and err is fitting error. The approximation of f will be proposed using the fitted second order polynomial regression model, called the quadratic model. The quadratic model of f can be written as following (Montgomery & Peck, 1992).

$$Y = b_0 + \sum_{i=1}^{k} b_i X_i + \sum_{i=1}^{k} b_{ii} X_i^2 + \sum_{i=1}^{k} b_{ij} X_i X_j \pm err \tag{2}$$

where Y is the corresponding response and X_i are the values of the ith machining process parameters. The terms $b\ldots$. are the regression coefficients and the residual err measures the experimental error of the observations. This assumed surface Y contains linear, squared and cross product terms of parameters X_i's. In order to estimate the regression coefficients a number of experimental design techniques are available. Box and Hunter (1957) have proposed that scheme based on central composite rotatable design fits the second order response surface very accurately. Let the points (0, 0 ….0) represent the centre of the region in which the relation between Y and X is under investigation. From the result of any experiment the standard error, err of Y can be computed at any point on the fitted surface. This standard error will be a function of the co-ordinates X_i's of the point. Due to rotatability condition this standard error is same at all equidistance points with the distance ρ from the centre of the region i.e. for all points for which (Cochran & Cox, 1962):

$$X_1^2 + X_2^2 + \cdots + X_k^2 = \rho^2 = \text{ Constant} \tag{3}$$

The components of Central Composite Second Order Rotatable Design for different number of variables are shown in Table 4.

Table 4

Face centered central composite design matrix

Exp. No.	Actual Variables		
	Cutting Speed, s (m/min)	Feed rate, f(mm/rev)	Depth of cut, d (mm)
1	-1	-1	-1
2	+1	-1	-1
3	-1	+1	-1
4	+1	+1	-1
5	-1	-1	+1
6	+1	-1	+1
7	-1	+1	+1
8	+1	+1	+1
9	$-\alpha$	0	0
10	$+\alpha$	0	0
11	0	$-\alpha$	0
12	0	$+\alpha$	0
13	0	0	$-\alpha$
14	0	0	$+\alpha$
15	0	0	0
16	0	0	0
17	0	0	0
18	0	0	0
19	0	0	0
20	0	0	0

Design Expert Software version 7.0 is used to develop the experimental plan for RSM. During machinability study, the machining parameters such as the cutting speed (s), feed rate (f) and depth of cut (d) are selected as the independent input variables. The desired responses are the surface roughness (Ra) and tool wear (VBc) which are assumed to be affected by the above three principal machining parameters. The response surface methodology is engaged for modeling and analyzing the machining parameters in the turning process so as to obtain the machinability performances in terms of surface roughness (Ra) and flank wear (VBc). A rotatable central composite design is selected for the experimentations. It is the most extensively used experimental design for the modeling a second - order response surface. For a given number of variables, the required to achieve ratability is computed where n_f is the number of points in the 2k factorial design (k is the number of factors). Rotability refers to the uniformity of prediction error. In rotatable designs, all points at the same radial distance (r) from the center point have the same magnitude of prediction error. A rotatable CCD consists of 2k fractional factorial points, augmented by 2k axial points and n_c, centre points (0, 0, 0, 0…, 0) the centre points vary from three to six. In this experimentation, eight (2x3) factorial points, six axial points (2x3) and six centre runs, a total of 20 experimental runs have been considered. A randomized experimental run has been carried out to minimize the error due to machining set-up and the regression models were obtained and analyzed using analysis of variance (ANOVA).

4. Results and discussion

4.1 Experimental data

The turning experiments were conducted, with three levels of cutting parameters as provided in Table 3 to investigate the their effect on the surface roughness and tool wear as the responses. The experimental data are presented in Table 5.

Table 5
Experimental results obtained in machining Al-Si alloy and composite samples

Exp No	Cutting Speed (s), m/min	Feed (f), (mm/rev)	Depth of Cut (d in mm)	Surface Roughness (SR in µm)		Tool Wear (TW in mm)	
				Al-Si	AMC	Al-Si	AMC
1	-1	-1	-1	1.98	1.38	0.052	0.072
2	+1	-1	-1	1.43	1.12	0.132	0.151
3	-1	+1	-1	5.15	4.68	0.079	0.098
4	+1	+1	-1	2.89	2.23	0.203	0.223
5	-1	-1	+1	2.1	1.63	0.051	0.069
6	+1	-1	+1	1.72	1.25	0.139	0.160
7	-1	+1	+1	5.32	4.85	0.081	0.098
8	+1	+1	+1	3.37	2.9	0.205	0.226
9	$-\alpha$	0	0	4.44	3.97	0.034	0.073
10	$+\alpha$	0	0	2.67	2.2	0.217	0.285
11	0	$-\alpha$	0	0.85	0.38	0.088	0.1
12	0	$+\alpha$	0	4.74	4.23	0.128	0.197
13	0	0	$-\alpha$	2.04	1.57	0.108	0.121
14	0	0	$+\alpha$	2.49	2.02	0.116	0.127
15	0	0	0	3.46	2.99	0.104	0.116
16	0	0	0	3.46	2.99	0.105	0.121
17	0	0	0	3.48	3.01	0.104	0.119
18	0	0	0	3.46	2.99	0.103	0.114
19	0	0	0	3.46	2.99	0.105	0.115
20	0	0	0	3.46	2.99	0.104	0.116

4.2 Multiple regression predictive models for surface roughness and tool wear

4.2.1 Selection of adequate model

The adequacy of the model for Al-Si Alloy and AMC prepared with fly ash, was decided by performing sequential model sum of squares. Table 6 and Table 7 show the sequential model sum of squares test data for two different materials to select an adequate model to fit the surface roughness and tool wear. The sequential model sum of squares test in each table shows, how the terms of increasing complexity contribute to the model. Results from Tables 6 and Table 7 indicated quadratic models for surface roughness and tool wear of the test samples.

Table 6
Selection of adequate model for surface roughness

Sequential Model Sum of squares (Al-Si Alloy)						
Source	Sum of Squares	df	Mean Square	F Value	p-value Prob > F	
Mean vs Total	192.014	1	192.014			
Linear vs Mean	23.90991	3	7.96997	29.612	< 0.0001	
2FI vs Linear	1.3808	3	0.460267	2.045248	0.1572	
Quadratic vs 2FI	2.793803	3	0.931268	70.68854	< 0.0001	Suggested
Cubic vs Quadratic	0.050441	4	0.01261	0.930622	0.5050	Aliased
Residual	0.081302	6	0.01355			
Total	220.2303	20	11.01152			
Sequential Model Sum of squares (MMC-UFA)						
Mean vs Total	137.1308	1	137.1308			
Linear vs Mean	23.16737	3	7.722456	25.57164	< 0.0001	
2FI vs Linear	1.8117	3	0.6039	2.599409	0.0967	
Quadratic vs 2FI	2.865819	3	0.955273	61.88273	< 0.0001	Suggested
Cubic vs Quadratic	0.085682	4	0.02142	1.871157	0.2348	Aliased
Residual	0.068686	6	0.011448			
Total	165.1301	20	8.256505			

Table 7
Selection of adequate model for tool wear

Sequential model sum of squares (Al-Si Alloy)						
Source	Sum of Squares	df	Mean Square	F Value	p-value Prob > F	
Mean vs Total	0.254928	1	0.254928			
Linear vs Mean	0.043396	3	0.014465	97.99664	< 0.0001	Suggested
2FI vs Linear	0.000809	3	0.00027	2.255564	0.1303	
Quadratic vs 2FI	0.001001	3	0.000334	6.045833	0.0129	Suggested
Cubic vs Quadratic	0.000537	4	0.000134	55.37661	< 0.0001	Aliased
Residual	1.46E-05	6	2.43E-06			
Total	0.300686	20	0.015034			
Sequential model sum of squares (AMC)						
Mean vs Total	0.36477	1	0.36477			
Linear vs Mean	0.05381	3	0.017937	36.57428	< 0.0001	
2FI vs Linear	0.00089	3	0.000297	0.554644	0.6541	
Quadratic vs 2FI	0.005736	3	0.001912	15.66187	0.0004	Suggested
Cubic vs Quadratic	0.000427	4	0.000107	0.806275	0.5637	Aliased
Residual	0.000794	6	0.000132			
Total	0.426427	20	0.021321			

4.2.2 Analysis of variance

The adequacy of the developed models are tested at 95% confidence interval using the ANOVA technique, and the results of the quadratic order response surface model fitting in the form of ANOVA are given in Tables 8 and 9 for surface roughness and Tables 10 and 11 for tool wear in the tested Al-Si alloy and composite specimens respectively. Tables 8, 9, 10 and 11 show the values of coefficient of determination R^2 are nearly equal to 1. The adjusted coefficient of determination R^2 is variation of the ordinary R^2 statistic that reflects the number of factors in the model. The entire adequacy measures are closer to 1, which is in reasonable agreement and indicate adequate models. The adequate precision 'Adeq Precision' compares the range of the predicted value at the design points to the average prediction error. Adequate precision measures signal to noise ratio. In the present data, the value of adequate precision is significantly greater than 4 which are desirable. The adequate precision ratio above 4 indicates adequate model discrimination. The experimental data also reveals an improved precision and reliability of the conducted experiments. Prediction error sum of squares (PRESS)values are considerably small.

Table 8
ANOVA results for Al-Si Alloy (surface roughness)

Source	Sum of	df	Mean	F	p-value	
Model	28.08451	9	3.120501	236.8639	< 0.0001	significant
A-s	4.824098	1	4.824098	366.1766	< 0.0001	significant
B-f	18.84412	1	18.84412	1430.376	< 0.0001	significant
C-d	0.241695	1	0.241695	18.34599	0.0016	significant
AB	1.3448	1	1.3448	102.078	< 0.0001	significant
AC	0.0288	1	0.0288	2.186084	0.1701	
BC	0.0072	1	0.0072	0.546521	0.4767	
A^2	0.062793	1	0.062793	4.766345	0.0540	
B^2	0.592071	1	0.592071	44.94155	< 0.0001	significant
C^2	2.192797	1	2.192797	166.4458	< 0.0001	significant
Residual	0.131742	10	0.013174			
Lack of Fit	0.131409	5	0.026282			
Pure Error	0.000333	5	6.67E-05			
Cor Total	28.21626	19				

R-Squared= 0.99533 Std. Dev.= 0.11477 Adj R-Squared= 0.99112 Mean= 3.0985
Pred R-Squared= 0.96461 C.V. %= 3.70434 Adeq Precision= 53.03167 PRESS= 0.99856

Tables 8, 9, 10 and 11 also presents that the values of 'Probability > F' in for all models are less than 0.0500, indicate that all the models are significant. The 'Lack-of-fit' value implies that the 'Lack-of-fit' is not significant relative to the pure error. From the above analysis, it has been asserted that the developed models are well within the limits and can be used for the prediction of responses.

Table 9
ANOVA results for Aluminum alloy matrix composite (surface roughness)

Source	Sum of	df	Mean	F	p-value	
Model	27.84489	9	3.093876	200.4218	< 0.0001	significant
A-s	4.705963	1	4.705963	304.853	< 0.0001	significant
B-f	18.17527	1	18.17527	1177.396	< 0.0001	significant
C-d	0.286139	1	0.286139	18.53616	0.0015	significant
AB	1.7672	1	1.7672	114.4795	< 0.0001	significant
AC	0.01805	1	0.01805	1.169282	0.3049	
BC	0.02645	1	0.02645	1.713435	0.2198	
A^2	0.057709	1	0.057709	3.738429	0.0820	
B^2	0.650704	1	0.650704	42.15268	< 0.0001	significant
C^2	2.223579	1	2.223579	144.0438	< 0.0001	significant
Residual	0.154368	10	0.015437			
Lack of Fit	0.154035	5	0.030807			
Pure Error	0.000333	5	6.67E-05			
Cor Total	27.99926	19				

R-Squared= 0.99448　　　　Std. Dev.= 0.12424　　　　　　　Adj R-Squared= 0.98952　　Mean= 2.6185

Pred R-Squared=0.95561　　C.V. %= 4.74489　　　　　　　Adeq Precision= 49.67930　PRESS= 1.24281

Table 10
ANOVA results for Al-Si alloy (tool wear)

Source	Sum of Squares	df	Mean Square	F Value	p-value Prob > F	
Model	0.045206	9	0.005023	90.98923	< 0.0001	significant
A-s	0.038357	1	0.038357	694.8432	< 0.0001	significant
B-f	0.004998	1	0.004998	90.54672	< 0.0001	significant
C-d	4.03E-05	1	4.03E-05	0.729683	0.4130	
AB	0.0008	1	0.0008	14.49201	0.0034	significant
AC	8E-06	1	8E-06	0.14492	0.7114	
BC	5E-07	1	5E-07	0.009058	0.9261	
A^2	0.00091	1	0.00091	16.48645	0.0023	significant
B^2	4.46E-05	1	4.46E-05	0.808317	0.3898	
C^2	0.000145	1	0.000145	2.62973	0.1359	
Residual	0.000552	10	5.52E-05			
Lack of Fit	0.000549	5	0.00011			
Pure Error	2.83E-06	5	5.67E-07			
Cor Total	0.045758	19				

R-Squared = 0.98793　　　　Std. Dev.= 0.00742　　　　　　Adj R-Squared=0.97707　　Mean=0.1129

Pred R-Squared=0.90846　C.V. %= 6.58092　　　　　　　Adeq Precision= 33.93013　PRESS= 0.00418

Table 11
ANOVA results for Al-Si alloy matrix composite (tool wear)

Source	Sum of Squares	df	Mean Square	F Value	p-value Prob > F	
Model	0.060436	9	0.006715	55.00972	< 0.0001	significant
A-s	0.044497	1	0.044497	364.5111	< 0.0001	significant
B-f	0.009287	1	0.009287	76.07826	< 0.0001	significant
C-d	2.67E-05	1	2.67E-05	0.218615	0.6501	
AB	0.000861	1	0.000861	7.054249	0.0241	significant
AC	2.81E-05	1	2.81E-05	0.230397	0.6416	
BC	1.13E-06	1	1.13E-06	0.009216	0.9254	
A^2	0.005053	1	0.005053	41.39707	< 0.0001	significant
B^2	0.000909	1	0.000909	7.447262	0.0212	significant
C^2	7.46E-06	1	7.46E-06	0.061133	0.8097	
Residual	0.001221	10	0.000122			
Lack of Fit	0.001186	5	0.000237			
Pure Error	3.48E-05	5	6.97E-06			
Cor Total	0.061657	19				

R-Squared= 0.98020	Std. Dev.= 0.01104	Adj R-Squared= 0.96238	Mean= 0.13505
Pred R-Squared= 0.85343	C.V. %= 8.18112	Adeq Precision= 25.07484	

4.2.3 The developed predictive model

The normal probability plots as shown in Figs. 5 and 6 for the surface roughness and Figs. 7 and 8 for the tool wear reveals that the residuals fall in a straight line i.e, the errors are distributed normally.
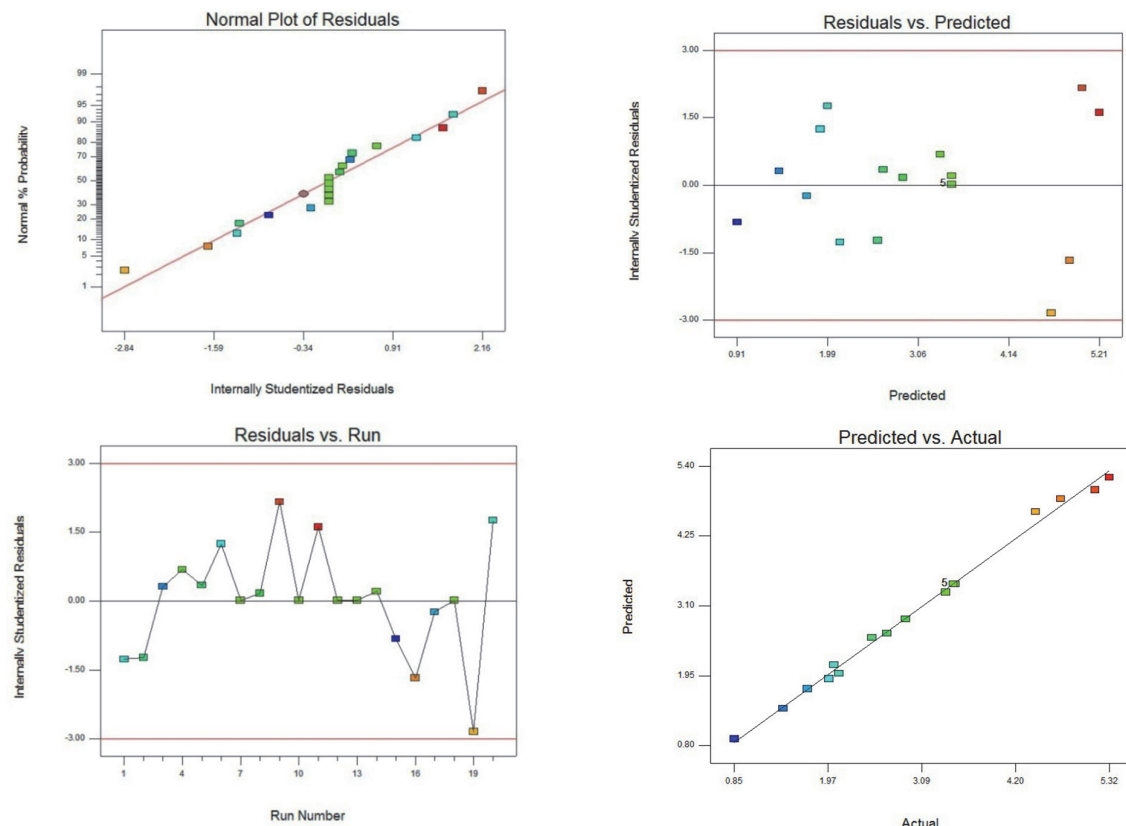
Fig. 5. Residual plots for surface roughness of post turning Al-Si alloy specimen
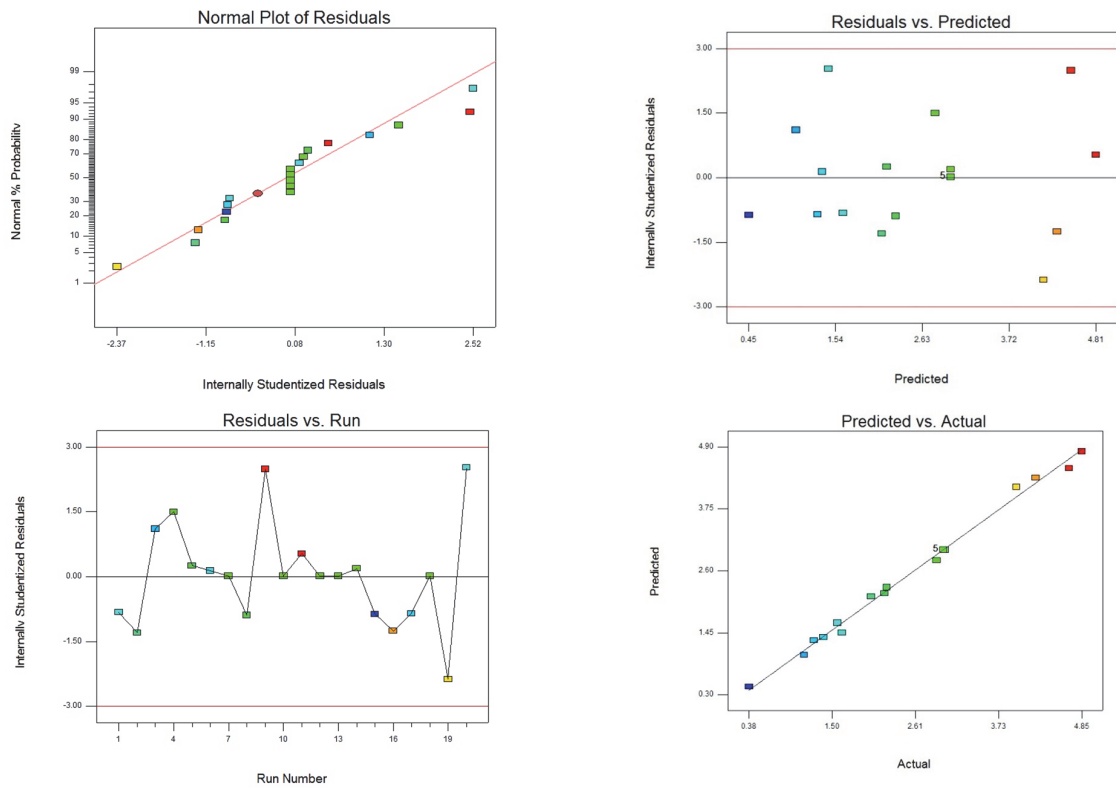
**Fig. 6.** Residual plots for surface roughness of post turning composite specimen
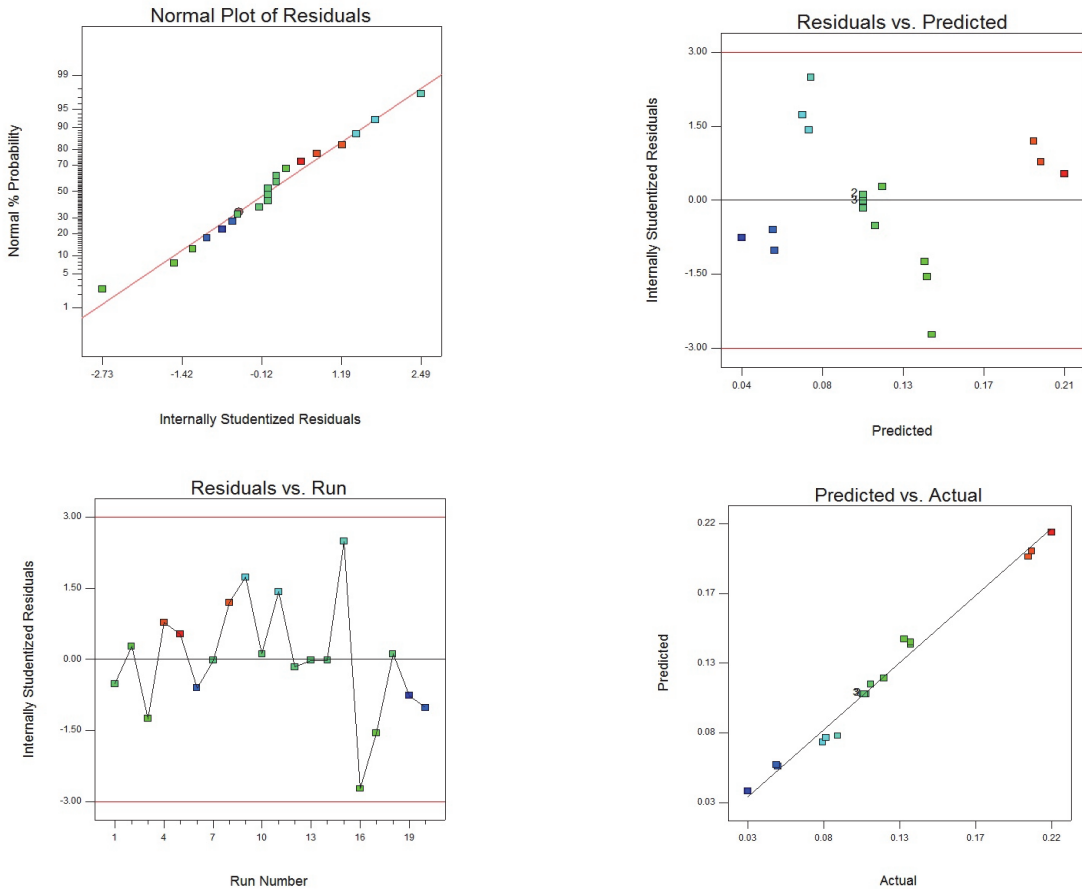
**Fig. 7.**Residual plots for tool wear of post turning Al-Si alloy specimen
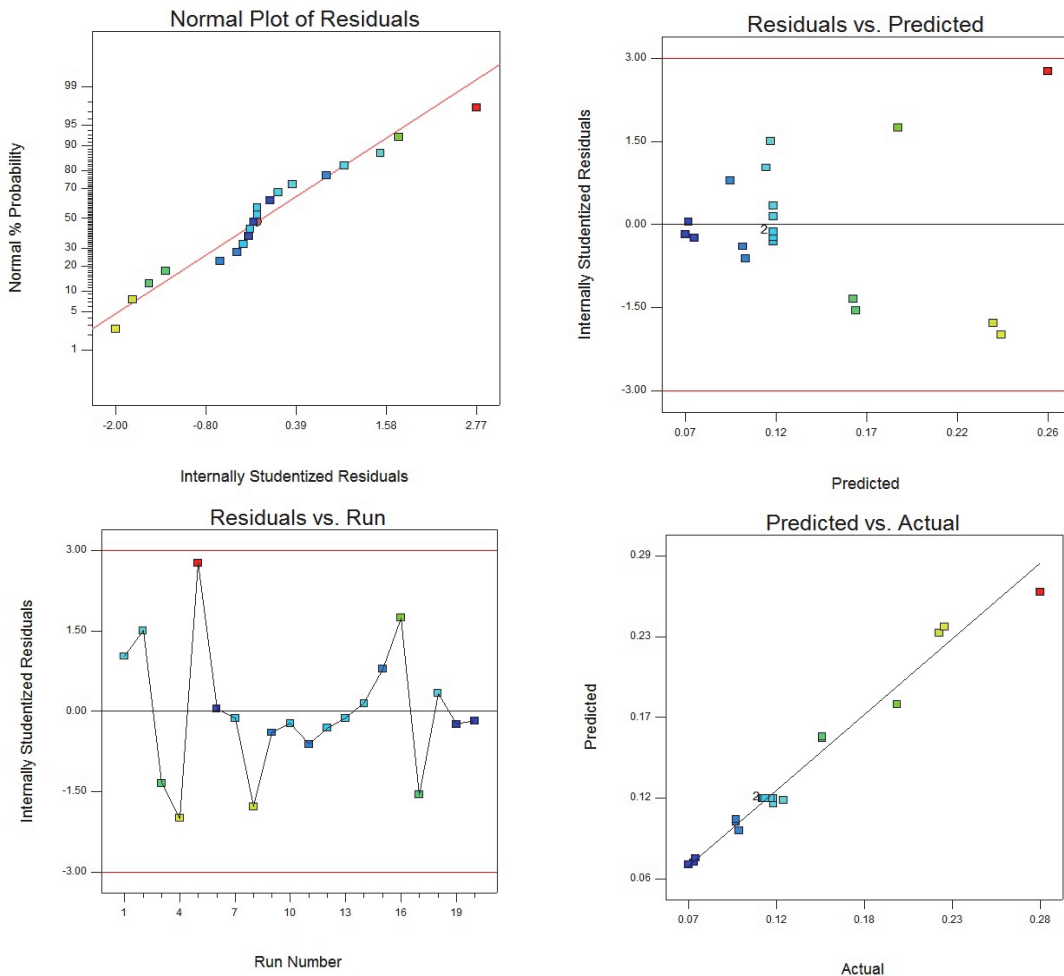
Fig. 8. Residual plots for tool wear of post turning composite specimen

The Independence of the data was tested, by plotting a graph between the residuals, and the run order for surface roughness and tool wear confirms that there is no predictable pattern observed, because all the run residues lay on or between the levels. The validity of these models was tested. For both the specimens, the predicted values of the response variables were fairly close to the corresponding experimental values. The models were adequate as represented by the points falling on a straight line in the normal probability plot. The errors were normally distributed confirmed a good-fit model. Also, the plot of the residuals versus the predicted surface roughness and tool wear is structure less i.e. containing no obvious pattern.

4.2.4 Multiple linear regression models

The surface roughness and tool wear models were developed by using the turning experiment data listed in Table 5 for the Al-Si Alloy and AMC.

Surface roughness models:

For Al-Si Alloy:

$$SR = 3.45 - 0.59s + 1.17f + 0.13d - 0.41sf + 0.06sd + 0.03fd + 0.06s^2 - 0.20f^2 - 0.39d^2$$

(4)

For AMC:

$$SR = 2.98 - 0.58s + 1.15f + 0.14d - 0.47sf + 0.04sd + 0.05fd + 0.06s^2 - 0.21f^2 - 0.39d^2$$

(5)

Tool wear models

For Al-Si Alloy:

$$VB_c = 0.104105 + 0.052997s + 0.019131f + 0.001717d + 0.010875sf + 0.00125sd \qquad (6)$$
$$-0.00025fd + 0.0007947s^2 + 0.00176f^2 + 0.003174d^2$$

For AMC:

$$VB_c = 0.117331 + 0.057081s + 0.026077f + 0.001398d + 0.010375sf + 0.001875sd \qquad (7)$$
$$-0.00037fd + 0.018726s^2 + 0.007942f^2 - 0.00072d^2,$$

where, *s* is cutting speed in the range between 90 m/min to 150 m/min, *f* is feed rate in the range between 0.07 mm/rev to 0.21 mm/rev, *d* is the depth of cut in the range between 0.2 mm to 0.6 mm and are the main effects of the process variables. The combined effect of process variables i.e. interaction between the process parameters such as *s* and *f*, *s* and *d* or *f* and *d* show quantitative affect of process parameters on the surface roughness of the materials. The main effect of feed rate and depth of cut (i.e. coefficient attached to *f* and *d*) are positive in values indicating that all these parameters increase surface roughness of the material. Whereas, the coefficient attached to cutting speed in value is negative. This means, it decreases surface roughness of the material. Out of the three parameters, feed rate has the greatest effect on the surface roughness of the material. The effect of feed is 2 fold higher in comparison to the effect of cutting speed and 9 fold higher in comparison to the effect of depth of cut, varied during the experiment. The surface roughness decreases with the increase in cutting speed up to certain level and the it increase with further increase in cutting speed, because of the creation of narrow grooves on the work piece. The temperature of the work piece has increased with the increase in cutting speed, which led to weaken the binding between the reinforcement and matrix. At higher value of feed and depth of cut the surface roughness of the material decreases. This is due to work hardening of the matrix material as well as confrontation of the rotating specimen with the debris produced by the chafing action of the bar against the carbide tool. For regression equation of the form $y = b_0 + b_1X_1 + b_2X_2 + ... + b_{12}X_1X_2 + b_{23}X_2X_3 + ... + b_1X^2{}_1 + b_2X^2{}_2 + ...b_nX_n^2$, y = response variable and $b_1, b_2.....b_n$ are regression coefficients attached with process variables. $y = b_0$, When $X_1, X_2.....X_n$ are 0.*b₀*is the response of the material when the operating parameters are at their zero level. The zero level is also expressed as base level around which the variables are varied at two levels i.e. the highest level and the lowest level. In the present work *s, f* and *d* are varied between 90 m/min- 150 m/min, 0.07 mm/rev – 0.21 mm/rev and 0.2 mm – 0.6 mm respectively. The first column in the above Table 5 indicates b_0 value, which are positive response i.e. surface roughness value due to dry machining when all the input parameters are kept at their base level i.e. (*s*= 120 m/min, *f*= 0.14 mm/rev and *d*=0.4 mm). Thus, if we insert 0 for *s, f* and *d* in equations, then the response of the three materials are expressed as surface roughness. That means for the combination of operating variables at *s* = 120 m/min, *f*= 0.14 mm/rev and *d*=0.4 mm , computed b₀ values are 3.45 for virgin Al-Si alloy in comparison to 2.98 for MMC reinforced with untreated fly ash.

Tables 12 and 13 show the experimental value at the base level as well as the value for b_0, calculated by using data shown in Table 5 for the surface roughness and tool wear respectively. It is observed from Tables 12 and 13, that there is a little difference between the experimental value and the calculated value. Thus, equations developed were accurate enough to predict amount of surface roughness and tool wear which would occur for any treatment combination of the process parameters in the range of variation of variables. The theoretical values and experimental values for surface roughness and tool wear are compared and reported in Tables 14 and 15.

Table 12

Regression equation coefficients for the alloy and composite (surface roughness)

Material	b_o	Main effect coefficient
Al-Si alloy	+3.45	$s= -0.59$ $f=+1.17$ $d= +0.13$
AMC	+2.98	$s= -0.58$ $f=+1.15$ $d= +0.14$

Table 13

Regression equation coefficients for the alloy and composite (tool wear)

Material	b_o	Main effect coefficient
Al-Si Alloy	+0.104	$s= +0.05229$ $f=+0.01913$ $d= +0.00171$
AMC	+0.117	$s= +0.05708$ $f=+0.02607$ $d= +0.00139$

Table 14

Comparative value of surface roughness for two materials at base level

Material	s (m/min)	f (mm/rev)	d (mm)	Theoretical value of Surface Roughness	Experimental value of Surface Roughness
Al-Si Alloy	120	0.14	0.4	+3.45	+3.46
AMC	120	0.14	0.4	+2.98	+2.99

Table 15

Comparative values of tool wear for two materials at base level

Material	s (m/min)	f (mm/rev)	d (mm)	Theoretical value of Flank wear	Experimental value of Flank wear
Al-Si Alloy	120	0.14	0.4	+0.104	+0.105
AMC	120	0.14	0.4	+0.117	+0.116

4.2.5 Confirmation test

Confirmation tests were conducted to validate the statistical analysis by selecting experimental conditions that are different from those employed in the analysis. The parameters used in the confirmation test for surface roughness and tool wear are presented in Tables 16 and 17.

Table 16

Parameters used in the confirmation test for surface roughness

Exp No	Cutting Speed(m/min)	Feed Rate (mm/rev)	Depth of cut (mm)
1	100	0.07	0.3
2	140	0.21	0.6

Table 17

Parameters used in the confirmation test for tool wear

Exp No	Cutting Speed(m/min)	Feed Rate (mm/rev)	Depth of cut (mm)
1	100	0.07	0.3
2	140	0.21	0.6

The results of the confirmation tests are presented in Table 18 and Table 19. Experimental results are compared with the computed values developed from the regression models. Table 18 and Table 19 reveal that the experimental values and calculated values from the regression equation are nearly the same with the least error (±5%). The resulting equations are capable of predicting the surface roughness and tool flank wear to an acceptable level of accuracy.

Table 18
Results of the confirmation test for surface roughness

Material	Experiment-1			Experiment-2		
	Surface Roughness(Ra)			Surface Roughness(Ra)		
	Model	Experiment	Error (%)	Model	Experiment	Error(%)
Al-Si Alloy	2.10	2.06	1.90	3.60	3.71	-3.05
AMC	2.27	2.32	-2.20	3.09	2.98	3.55

Table 19
Results of the confirmation test for tool wear

Material	Experiment-1			Experiment-2		
	Flank wear (VB_c)			Flank wear (VB_c)		
	Model	Experiment	Error (%)	Model	Experiment	Error (%)
Al-Si Alloy	0.062	0.064	-3.2	0.176	0.171	2.8
MMC(UFA)	0.075	0.072	4.0	0.204	0.197	3.4

Machined surface morphology of virgin Al-Si alloy and AMC reinforced with as received fly ash were examined by the optimum process parameters with the help of scanning electron microscope (SEM: JEOL, Model - JSM-6510) to reveal the surface texture as depicted in Fig. 9 and Fig. 10. The SEM image of the machined surface of the AMC reinforced with fly ash reveals that a relatively better surface finish is achieved compared with that of virgin Al-Si alloy, which has large feed marks. Given that the chips are broken by dispersed reinforcement particles during the machining of AMC composite at optimum conditions, the entrapment of chips between the work piece and tool was avoided. Therefore, BUE formation on the tool is prevented and the surface finish was enhanced.
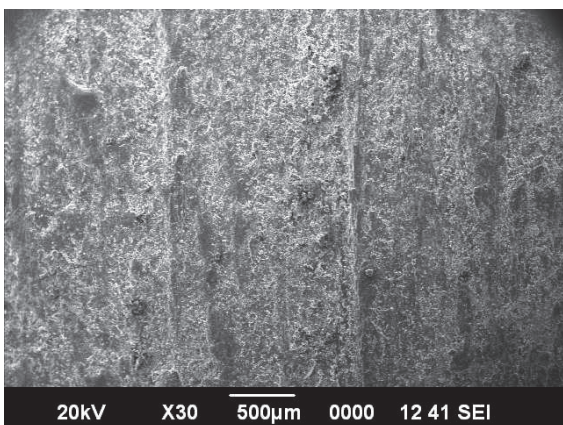
Fig. 9. SEM image of Al-Si alloy after machining
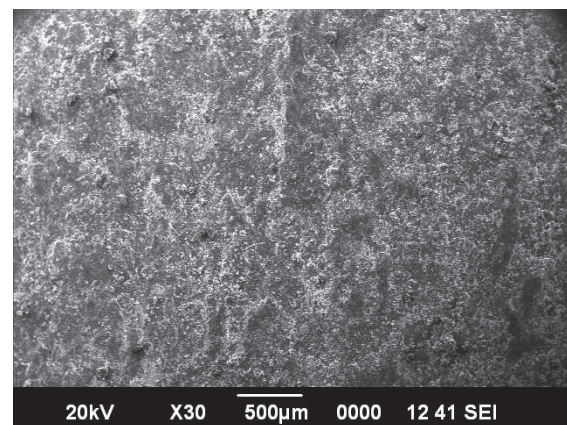
Fig. 10. SEM image of composite after machining

The fly ash particles however are much smaller in size compared to size of chips in pure Al-Si alloy and hence do not cause much damage to the surface. Reddy et. al. (2013), Shanmughasundaram and Subramanian (2013) reported that the presence of the reinforcement enhances the machinability in terms of both surface roughness and lower tendency to clog the cutting tool, when compared to a non-reinforced Al alloy.

5. Conclusions

1. The metal matrix composite prepared with waste fly ash has shown better machining performance in comparison to that for virgin Al-Si alloy.
2. Low values of surface roughness and tool wear were obtained for AMC at all test conditions in comparison to that of Al-Si alloy.
3. Multiple regression predictive models were developed to predict the machining responses such as surface roughness and tool wear of the AMC reinforced with waste fly ash. Good agreements between the predicted and actual responses were observed.
4. ANOVA results indicated that the values of coefficient of determination R^2 were nearly equal to 1. The adjusted coefficient of determination R^2 was variation of the ordinary R^2 statistic that reflected the number of factors in the model. The entire adequacy measured was closer to 1, which was in reasonable agreement and indicated adequate models.
5. Confirmation experiments revealed that the experimental values and calculated values from the regression equation are nearly the same with the least error (±5%). The resulting equations are capable of predicting the surface roughness and tool flank wear to an acceptable level of accuracy.
6. The SEM image of the machined surface for AMC reported a relatively better surface finish compared to that of virgin Al-Si alloy, which had large feed marks.

References

Anasyida, A. S., Daud, A. R., & Ghazali, M. J. (2010). Dry sliding wear behavior of Al–12Si–4Mg alloy with cerium addition. *Materials and Design*, *31*(1), 365-374.

Banerjee, S., Mahapatro, D., & Dubey, S. (2009). Some study on electrical discharge machining of ({WC+ TiC+ TaC/NbC}–Co) cemented carbide. *The International Journal of Advanced Manufacturing Technology*, *43*(11-12), 1177-1188.

Bienia, J., Walczak, M., Surowska, B., & Sobczaka, J. (2003). Microstructure and corrosion behavior of aluminum fly ash composites. *Journal of Optoelectronics and Advanced Materials*, 5(2), 493-502.

Box, G. E., & Hunter, J. S. (1957). Multi-factor experimental designs for exploring response surfaces. *The Annals of Mathematical Statistics*, *28*(1), 195-241.

Charles, S., Arunachalam, V. P., & Subramanian, R. (2006). Property analysis and mathematical modeling of machining parameters of aluminum hybrid composites fabricated by powder metallurgy. *Journal of Advanced Materials*, *38*(4), 25-34.

Cochran, W. G., & Cox, G. M.(1957). *Experimental Designs*. John Wiley and Sons, New York.

Dou, Z., Wu, G., Huang, X., Sun, D., & Jiang, L. (2007). Electromagnetic shielding effectiveness of aluminum alloy–fly ash composites. *Composites Part A: Applied Science and Manufacturing*, *38*(1), 186-191.

Li, X., & Seah, W. K. H. (2001). Tool wear acceleration in relation to workpiece reinforcement percentage in cutting of metal matrix composites. *Wear*, *247*(2), 161-171.

Manna, A., & Bhattacharayya, B. (2005). Influence of machining parameters on the machinability of particulate reinforced Al/SiC–MMC. *The International Journal of Advanced Manufacturing Technology*, *25*(9), 850-856.

Mishra, P., Das, D., Ukamanal, M., Routara, B., & Sahoo, A. (2015). Multi-response optimization of process parameters using Taguchi method and grey relational analysis during turning AA 7075/SiC composite in dry and spray cooling environments. *International Journal of Industrial Engineering Computations*, *6*(4), 445-456.

Montgomery, D.C. (1990). *Introduction to statistical quality control*. Wiley, New York.

Montgomery, D. C. & Peck, E. A. (1992). *Introduction to linear regression analysis,* Wiley, New York.

Prakash, J. U., Moorthy, T. V., & Peter, J. M. (2013). Experimental investigations on machinability of aluminium alloy (A413)/Flyash/B_4C hybrid composites using wire EDM. *Procedia Engineering*, *64*, 1344-1353.

Rao, C. P., Bhagyashekar, M. S., & Viswanath, N. (2014). Machining behavior of Al6061-flyash composites. *Procedia Materials Science*, *5*, 1593-1602.

Reddy, S. M., Chetty, S. V., & Premkumar, S. (2013). Evaluation of mechanical and wear properties of Al 7075, flyash and E-glass fibre-reinforced hybrid metal matrix composites. *Indian Foundry Journal*, *59*(2), 27-32.

Rohatgi, P. K., Kim, J. K., Gupta, N., Alaraj, S., & Daoud, A. (2006). Compressive characteristics of A356/fly ash cenosphere composites synthesized by pressure infiltration technique. *Composites Part A: Applied Science and Manufacturing, 37*(3), 430-437.

Rohatgi, P. K., Gajdardziska-Josifovska, M., Robertson, D. P., Kim, J. K., & Guo, R. Q. (2002). Age-hardening characteristics of aluminum alloy-hollow fly ash composites. *Metallurgical and Materials Transactions A*, *33*(5), 1541-1547.

Rohatgi, P. K., Weiss, D., & Gupta, N. (2006). Applications of fly ash in synthesizing low-cost MMCs for automotive and other applications. *JOM*, *58*(11), 71-76.

Saheb, N., Laoui, T., Daud, A. R., Harun, M., Radiman, S., & Yahaya, R. (2001). Influence of Ti addition on wear properties of Al–Si eutectic alloys. *Wear*, *249*(8), 656-662.

Sahoo, A. K., Pradhan, S., & Rout, A. K. (2013). Development and machinability assessment in turning Al/SiCp-metal matrix composite with multilayer coated carbide insert using Taguchi and statistical techniques. *Archives of Civil and Mechanical Engineering*, *13*(1), 27-35.

Senapati, A. K., Mishra, P. C., Routray, B. C., & Ganguly, R. I. (2015). Mechanical behavior of aluminium matrix composite reinforced with untreated and treated waste fly ash. *Indian Journal of Science and Technology*, *8*(S9), 111-118.

Shanmughasundaram, P., & Subramanian, R. (2013). Wear behavior of eutectic Al-Si alloy-graphite composites fabricated by combined modified two-stage stir casting and squeeze casting methods. *Advances in Materials Science and Engineering*, 2013.

Shanmughasundaram, P., & Subramanian, R. (2013). Influence of graphite and machining parameters on the surface roughness of Al-fly ash/graphite hybrid composite: a Taguchi approach. *Journal of Mechanical Science and Technology*, *27*(8), 2445-2455.

Surappa, M. K. (2008). Synthesis of fly ash particle reinforced A356 Al composites and their characterization. *Materials Science and Engineering*: *A*, *480*(1), 117-124.

Wu, G. H., Dou, Z. Y., Jiang, L. T., & Cao, J. H. (2006). Damping properties of aluminum matrix–fly ash composites. *Materials Letters*, *60*(24), 2945-2948.

18